universität wien

MASTERARBEIT | MASTER'S THESIS

Titel | Title

Molecular Dynamics Simulation of the Gβ1γ2 M101V Mutation Associated to GNB1 Encephalopathy

verfasst von | submitted by

Lina Lindorfer BSc

angestrebter akademischer Grad | in partial fulfilment of the requirements for the degree of

Magistra pharmaciae (Mag. pharm.)

Wien | Vienna, 2026

Studienkennzahl lt. Studienblatt | Degree programme code as it appears on the student record sheet:	UA 066 605
Studienrichtung lt. Studienblatt | Degree programme as it appears on the student record sheet:	Masterstudium Pharmazie
Betreut von | Supervisor:	Assoz. Prof. Mag. Dr. Anna Weinzinger Privatdoz.

Acknowledgements

First and foremost, I would like to express my sincere gratitude to Assoc.-Prof. Mag. Dr. Anna Weinzinger, Privatdoz., for welcoming me into her research group and for her supervision throughout this master's thesis. I am very grateful for the opportunity to be part of such a supportive and inspiring research environment. I would also like to thank Ilia Steshin for his guidance, valuable input, and patience during this project. I truly appreciate his willingness to help and his support whenever assistance was needed. I am deeply thankful to my family and friends for their constant encouragement, understanding, and unconditional support. Without you, this journey would not have been possible. I am incredibly grateful to have such a strong and supportive network. Thank you all.

Abstract

GNB1 encephalopathy is a very rare neurodevelopmental disorder caused by pathogenic variants in the GNB1 gene, which encodes the Gβ1 subunit of heterotrimeric G proteins. Among all known variants, the M101V mutation has been reported in only two individuals and its molecular consequences remain poorly understood. In this study, molecular dynamics (MD) simulations were conducted to investigate the structural and thermodynamic effects of the M101V substitution within the Gβ1γ2 complex. These simulations were performed for both the wild-type and mutant form based on the PDB structure 4KFM. The impact of the mutation on protein stability and dynamic behaviour was then assessed with analyses including calculations for the change in free energy upon mutation (ΔΔG), root mean square deviation (RMSD) and root mean square fluctuation (RMSF) and also residue-residue and interaction analyses.

The free energy calculations revealed an average ΔΔG of 4,15 kJ/mol, indicating a slightly destabilizing effect of the mutation on the folded Gβ1γ2 complex. Despite this modest destabilization, RMSD and RMSF analyses showed high structural similarity between wild-type and mutant forms. Interaction analyses demonstrated reduced solvation energy for the mutant due to a minor decrease in polarity, while residue-residue analyses remained largely unchanged. These findings suggest that M101V preserves global structural integrity but finely alters the local hydrophobic environment, potentially influencing the interaction of Gβ1γ2 with downstream effectors like GIRK or AC5.

Overall, this work provides a framework for understanding how the M101V variant may contribute to GNB1 encephalopathy despite only minor structural perturbations. The results highlight the value of MD simulations for characterizing disease-associated variants and emphasize the need for future studies incorporating effector proteins and experimental validation to fully elucidate the functional consequences of this mutation.

Zusammenfassung

Die GNB1-Enzephalopathie ist eine sehr seltene neurologische Entwicklungsstörung, die durch pathogene Varianten im GNB1-Gen verursacht wird, welches für die Gβ1-Untereinheit heterotrimerer G-Proteine kodiert. Von allen bekannten Varianten wurde die M101V-Mutation bisher nur bei zwei Personen festgestellt, und ihre molekularen Auswirkungen sind noch weitgehend unverstanden. In dieser Studie wurden Molekulardynamik-Simulationen (MD) durchgeführt, um die strukturellen und thermodynamischen Auswirkungen der M101V-Substitution innerhalb des Gβ1γ2-Komplexes zu untersuchen. Diese Simulationen wurden sowohl für die Wildtyp- als auch für die Mutantenform auf der Grundlage der PDB-Struktur 4KFM durchgeführt. Die Auswirkungen der Mutation auf die Proteinstabilität und das dynamische Verhalten wurden dann mit Analysen bewertet, darunter Berechnungen der Änderung der freien Energie bei Mutation (ΔΔG), der quadratischen Mittelwertabweichung (RMSD) und der quadratischen Mittelwertfluktuation (RMSF) sowie Residuum-Residuum- und Interaktionsanalysen.

Die Berechnungen der freien Energie ergaben einen durchschnittlichen ΔΔG-Wert von 4,15 kJ/mol, der auf eine leicht destabilisierende Wirkung der Mutation auf den gefalteten Gβ1γ2-Komplex hindeutet. Trotz dieser geringen Destabilisierung zeigten die RMSD- und RMSF-Analysen eine hohe strukturelle Ähnlichkeit zwischen Wildtyp- und Mutantenform. Interaktionsanalysen zeigten eine verringerte Solvatationsenergie für die Mutante aufgrund einer geringfügigen Abnahme der Polarität, während die Residuum-Residuum-Analysen weitgehend unverändert blieben. Diese Ergebnisse deuten darauf hin, dass M101V die Grundstruktur bewahrt, aber die lokale hydrophobe Umgebung fein verändert, was möglicherweise die Interaktion von Gβ1γ2 mit nachgeschalteten Effektoren wie GIRK oder AC5 beeinflusst.

Insgesamt liefert diese Arbeit einen Rahmen für das Verständnis, wie die M101V-Variante trotz nur geringfügiger struktureller Störungen zur GNB1-Enzephalopathie beitragen kann. Die Ergebnisse unterstreichen den Wert von MD-Simulationen für die Charakterisierung krankheitsassoziierter Varianten und betonen die Notwendigkeit weiterer Studien unter Einbeziehung von Effektorproteinen und experimenteller Validierung, um die funktionellen Folgen dieser Mutation vollständig aufzuklären.

Inhaltsverzeichnis

Inhalt

List of abbreviations

AC5	Adenylyl cyclase 5
ADHD	Attention-deficit/hyperactivity disorder
ASD	Autism spectrum disorder
ATP	Adenosine triphosphate
BAR	Bennet's Acceptance Ratio
CFT	Crooks Fluctuation Theorem
CFT	Crooks Fluctuation Theorem
EEG	Electroencephalogram
GABA	γ-aminobutyric acid
GDD	Global development delay
GDP	Guanosine diphosphate
GIRK	G-protein-gated inward rectifier K^+ channels
GNB1	G protein subunit beta 1
GNB1-E	GNB1-encephalopathy
GPCR	G protein-coupled receptor
GPUs	Graphics processor units
GTP	Guanosine triphosphate
ID	Intellectual disability
LJ	Lennard-Jones
M	Methionine
MD	Molecular dynamics
MRI	Magnetic resonance imaging
NEMD	Non-equilibrium molecular dynamics
PDB	Protein Data Bank
PIP_2	Phosphatidylinositol 4,5-bisphosphate
RMSD	Root mean square deviation
RMSF	Root mean square fluctuation
SF	Selectivity filter
U	Potential energy
V	Valine
WT	Wild-type
ΔΔG	Change in Gibbs Free Energy

List of figures

List of tables

1 Literature Overview

1.1 GNB1 encephalopathy

GNB1-encephalopathy (GNB1-E) is considered a rare disease, affecting around 68 patients worldwide. Pathogenic variants in the G protein subunit beta 1 (GNB1) gene cause this disease. While most of these variants are de novo germline mutations, there are also cases where the mutation is inherited. (Nasvytis et al., 2024)

GNB1-E is a heterogeneous neurodevelopmental syndrome. Many different manifestations of the disease have been observed, but only one characteristic is present in all the known patients, which is global development delay (GDD). Additionally, more than half of patients experience intermediate to severe intellectual disability (ID), epilepsy, abnormal vision and muscle tone and gastrointestinal abnormalities. (Da Silva et al., 2021)

It is very likely that the mechanism of the disease is based on either the loss of function of the G protein through the inhibition of the interaction between Gβ1γ2 and downstream effectors. Or alternatively, it could be a gain of function due to a residue modification. Such a modification could hinder Gβ1γ2 binding to Gα, which would result in a consistently activated Gβ1γ2. (Petrovski et al., 2016)

1.1.1 Pathogenesis

G protein-coupled receptors (GPCRs) are membrane-bound proteins that detect external signals and transmit them into the cell via G proteins. These consist of three subunits: alpha (α), beta (β) and gamma (γ). (Nasvytis et al., 2024)

GNB1 is the gene that codes for the guanine nucleotide-binding protein subunit beta-1 (Gβ1). It is widely expressed throughout the body. The Gβ1 subunit is associated with the Gα and Gγ subunits of the heterotrimeric G protein, which play an essential role in the signaling cascade of G-protein-coupled receptors. (Petrovski et al., 2016) Gβ1 and Gγ2 are consistently connected, forming a dimer, while the Gα subunit is able to detach from the heterotrimer. (Reddy et al., 2021)

In their inactive state, the three subunits are bound together, and the α-subunit carries a guanosine diphosphate (GDP) molecule. When a GPCR is activated, GDP is exchanged for guanosine triphosphate (GTP), which triggers the breakdown of the trimer into Gα-GTP and Gβ1γ2. (Nasvytis et al., 2024) This leads to the release of Gβ1γ2, which can then interact with other proteins and trigger different signaling cascades. (Petrovski et al., 2016)

Examples of targets regulated by the dimer include most importantly G protein-gated inwardly rectifying K+ channels (GIRK1-4), but also presynaptic SNARE proteins, voltage-gated Ca^{2+} channels, some adenylyl cyclases, phosphoinositide 3 kinase gamma, phospholipase Cβ and G protein receptor kinases. (Reddy et al., 2021)

Lohmann et al. discovered that structural changes to the Gβ1-subunit resulting from pathogenic GNB1 variants can cause several disruptions. Either the Gβ1γ2 complex becomes unstable (loss of function), or the interaction with the α-subunit is impaired, which triggers constitutive activation of Gβ1γ2 (gain of function). Another possibility is that the binding of the Gαβ1γ2 trimer to the GPCR is altered. (Nasvytis et al., 2024)

The fact that GNB1 is functionally constrained indicates its critical biological role. It is therefore striking that multiple de novo missense mutations have been found in the gene. It is anticipated that approximately 77% of all simulated GNB1 variants will demonstrate non-synonymous effects, suggesting that GNB1 is under intense purifying selection. (Petrovski et al., 2016)

There are more than 25 mutations in the GNB1-gene causing GNB1-E, with the majority of mutations situated in exons 6 and 7 coding for amino acids 76 to 112 in Gβ1. (Reddy et al., 2021) 88% of all reported missense mutations are located in these regions of high mutation density, 49% in exon 6 and 39% in exon 7. These mutations are highly likely to interfere with the interaction site of the GNB1 protein. (Da Silva et al., 2021) In fact, exon 6, which makes up 6,4% of the GNB1 sequence, is known to be essential for the interaction between Gβ1γ2 and Gα. Different GNB1 mutations result in variable influences on the downstream pathway. (Petrovski et al., 2016)

1.1.2 Clinical manifestations

GNB1 encephalopathy (GNB1-E) is a neurodevelopmental disorder marked by moderate to severe developmental delays and intellectual disability, sometimes with structural abnormalities in the brain. Many patients also experience early-onset hypotonia and seizures. Additional symptoms that may occur include movement disorders like dystonia, visual and auditory impairments, behavioral abnormalities, feeding and growth issues, and gastrointestinal or genitourinary anomalies. (Revah-Politi et al., 2020)

Global Development Delay (GDD)

Global development delay is something that can be seen in every single case. Although there is no data on GNB1-1 in pregnancy, childbirth or newborns, the only known symptom in the very early stages is difficulty feeding. Later in childhood, development delay will become

noticeable. Children with GNB1-E are often late-starters when it comes to walking and often fail to walk independently. If they do walk, they usually develop gait disorders and fall frequently. Furthermore, hemiplegia, severe dyskinetic quadriplegia and spastic diplegia have also been reported in cases of GNB1-E. A lot of the patients are non-verbal, but if they can speak, their receptive language is less affected than their expressive language. Growth delay is also a common symptom resulting from GDD due to the inability to feed properly in early life. Usually, affected individuals catch up in height in later stages of life. (Nasvytis et al., 2024)

Intellectual disability (ID)

Roughly 75% of individuals diagnosed with GNB1 encephalopathy experience intellectual disabilities, ranging from mild to severe. It should be noted that some children are too young for an informative assessment of cognitive function, and the abilities of some older individuals were not properly documented. (Revah-Politi et al., 2020)

Muscle tone disorders

The neurological symptoms associated with GNB1-E can vary significantly in terms of type and severity. Hypotonia is the most frequent feature observed in early childhood, that in some cases persists, while in others it eventually develops into spastic hypertonia. A characteristic pattern that is often noted is increased muscle tone in the limbs combined with decreased axial tone. (Nasvytis et al., 2024)

Movement disorders

Movement disorders are common, with dystonia being the most frequently reported. These can range from minor dystonic finger posturing to generalized dystonia. Some patients also suffer from intermittent status dystonicus. (Nasvytis et al., 2024) Other movement abnormalities, such as myoclonus, chorea, athetosis and tics can also occur. (Jones et al., 2019)

Epilepsy

Epilepsy is observed in some of the patients. The seizure types involved include tonic, myoclonic, generalized tonic-clonic, absence and focal seizures. Epileptic spasms have also been reported. Several cases have been associated with West syndrome. In the early stages of life, an EEG may appear normal, but generalized or multifocal epileptiform discharges can develop over time, often during phases of deep sleep. (Revah-Politi et al., 2020)

Vision and Hearing

Abnormal eye movements, particularly nystagmus, are reported in over a third of patients. These disorders occur in various forms. These include horizontal, vertical, rotatory, or

alternating directions. (Nasvytis et al., 2024) In two individuals Hemati et al. reported improved eye movement ability over time. (Hemati et al., 2018) Additional findings include strabismus, upward gaze palsy, ophthalmoplegia, and disturbed ocular pursuit. Visual impairment can be characterized by symptoms such as cortical visual damage, optic nerve atrophy, and in some cases, rod-cone dystrophy. (Nasvytis et al., 2024)

Auditory deficits include unilateral or bilateral sensorineural hearing loss. In one patient, hypoplasia of the cochlear nerve combined with hearing loss was observable on the right side only. (Revah-Politi et al., 2020)

Behavior

Behavioral issues range from autism spectrum disorder (ASD) over attention-deficit/hyperactivity disorder (ADHD) to repetitive and stereotypic behaviors. (Revah-Politi et al., 2020)

Other Symptoms

Other observed features include gastrointestinal problems, genitourinary abnormalities in males, cardiovascular abnormalities, craniofacial anomalies, cutaneousmastocytosis, hypothyroidism and malignancy. (Revah-Politi et al., 2020)

1.1.3 Prognosis

Determining life expectancy is difficult due to the large number of children and young adults diagnosed with GNB1-E. Nevertheless, there are adult cases of GNB1-E patients, so it is definitely possible to reach adulthood and beyond. Based on the available data, it is only possible to speculate about the prognosis. Appropriate support and disease management can lead to a favorable outcome, since the symptoms do not go hand in hand with heightened morbidity and mortality. (Nasvytis et al., 2024)

1.1.4 Diagnostics

The primary challenge today is to identify the main disease-causing mutation. Due to advanced sequencing techniques, recognizing a mutation has become less of a problem, but it is not possible to say with certainty that a mutation that changes the protein sequence is the cause of a disease. Opposite, not all variants in a gene altering the protein sequence are necessarily pathogenic. (Lohmann et al., 2017)

Genetic testing is the only way to diagnose GNB1-E. The first-line diagnostic method is chromosomal microarray analysis (CMA). If this is inconclusive, next generation sequencing

can be used as an alternative. A diagnosis can be confirmed by identifying a pathogenic or likely pathogenic variant in the gene. (Nasvytis et al., 2024)

Currently, there are no laboratory markers indicating GNB1-E, despite various markers previously being assessed. Patients are encouraged to undergo an EEG to identify abnormal episodes or seizures. In addition, an MRI should be considered to detect potential abnormalities, although this is not present in every individual. (Nasvytis et al., 2024)

When only taking the phenotype into account, the symptoms do not clearly indicate GNB1-E. Therefore, all disorders involving ID and/or seizures should be considered in the differential diagnosis. These include Autosomal Dominant Intellectual Developmental Disorder, Autosomal Recessive Intellectual Developmental Disorder and Epileptic Encephalopathy. (Revah-Politi et al., 2020)

1.1.5 Treatment

Unfortunately, there are currently no guidelines available for treating GNB1-E. The existing options are based on previous cases and include deep brain stimulation, an intrathecal baclofen pump and various medications which are still in preclinical trials. These are considered to be the most promising. (Nasvytis et al., 2024)

Due to the wide range of symptoms observed in affected individuals, it is essential to involve a multidisciplinary approach to treatment from an early stage. Newborns may benefit from interventions such as feeding therapy, physiotherapy, and occupational therapy. Individualized plans are crucial as children grow. Support through physical rehabilitation, psychotherapy, and mobility aids is also recommended. (Nasvytis et al., 2024)

Seizures associated with GNB1 encephalopathy are managed using standard anti-epileptic drugs. No particular medication has been validated as superior through clinical trials. However, findings in animal models have shown promising results. These results were achieved using ethosuximide. (Nasvytis et al., 2024)

For movement disorders such as dystonia, treatment is based on existing protocols and includes anticholinergics, dopamine-related medications, benzodiazepines, and baclofen. Deep brain stimulation (DBS) is considered the most effective neuromodulation approach. Myoclonus was reduced by trihexyphenidyl, but agitation was induced. Dystonia was worsened by levodopa, and clonazepam showed little to no benefit. Other agents, such as risperidone, dantrolene, and phenobarbital also yielded limited positive results. (Nasvytis et al., 2024)

Physical and occupational therapy play a major role in preventing complications such as contractures and falls due to spasticity. When GNB1 mutations affect other systems, additional therapy by specialists is necessary to address those manifestations. (Nasvytis et al., 2024)

1.2 G-protein-gated inward rectifier (GIRK/Kir3.x)

G-protein-gated inward rectifier K^+ channels are mainly found in cardiac atrial tissue and in the central and peripheral nervous system. The task of these cells is to mediate various cellular actions initiated by neurotransmitters such as γ-aminobutyric acid (GABA), dopamine, serotonin, adenosine, enkephalin and somatostatin. These neurotransmitters bind to a variety of G-protein-coupled receptors, including muscarinic, opioid, dopamine and serotonin receptors. (Walsh, 2020) Upon dissociation from the GPCRs, Gβγ dimers then bind to GIRK channels, inducing their opening. (Lüscher and Slesinger, 2010)

Moreover, Kir3.x channels react to phosphatidylinositol-4,5-bisphosphate (PIP2), regulator G-protein signaling (RGS) proteins, phosphorylation, intracellular sodium and calcium ions and cholesterol. (Luo et al., 2022)

GIRK channels are involved in a variety of pathological conditions. This is due to their central role in controlling neuronal excitability. Dysregulation of GIRK signaling has been linked to neurological disorders such as schizophrenia and bipolar disorder. (Luo et al., 2022) Furthermore, due to its association with cell death and altered neuronal excitability, abnormal GIRK function has also been linked to epilepsy, Down's syndrome, Parkinson's disease and drug addiction. (Lüscher and Slesinger, 2010)

1.2.1 Structure

GIRK channels hyperpolarize neurons after the activation of several GPCRs. Their function varies significantly depending on the subunit composition. (Lüscher and Slesinger, 2010)

Kir3.x channels exist as both homo- and heterotetrameric complexes. The genes in mammalian cells that code for these subunits are GIRK1/Kir3.1, GIRK2/Kir3.2, GIRK3/Kir3.3, and GIRK4/Kir3.4. Each subunit features two transmembrane segments, a pore region, and cytoplasmic amino- and carboxyl-terminal domains. Of these domains, the cytoplasmic one tend to be the most divergent. (Luo et al., 2022)

The GIRK1 and GIRK3 subunits themselves cannot form homomers; however, they form heterotetrameric channel complexes, such as GIRK1/3 and GIRK2/3. GIRK2 is the only

channel that is capable of forming homotetramers. Nevertheless, GIRK2 can also form the heterotetramers GIRK1/2 and GIRK2/3. (Lüscher and Slesinger, 2010)

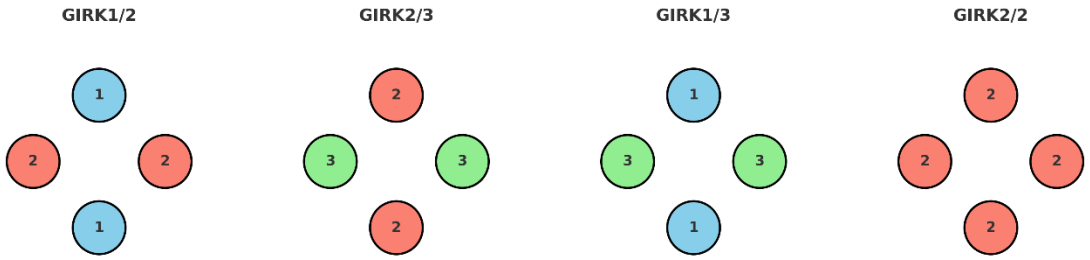

Figure 1 GIRK channel complexes. The three major GIRK subunits (GIRK1, GIRK2 and GIRK3) form heterotetramers (GIRK1/2, GIRK2/3 and GIRK1/3). GIRK2 is the only subunit able to form a homoteramer. GIRK4 is not considered a valuable subunit. (Lüscher and Slesinger, 2010) (figure created with ChatGPT)

GIRK1/3 is commonly found in the cerebral region. However, the predominant form appears to be GIRK1/2. GIRK2 is believed to play a vital role in generating GIRK currents. In contrast, GIRK4 is not considered to contribute to cerebral currents due to its low expression in the brain. Experiments with GIRK3-knockout mice yielded similar behavioral test results as wild-type mice, but the GIRK3-knockout mice experienced fewer withdrawal symptoms from sedatives and reduced cocaine use. This further suggests that GIRK3 is essential for GIRK signaling in the brain. Whether irregular variants, e.g. GIRK1/1/2/3, exist remains unknown. (Lüscher and Slesinger, 2010)

1.3 G-proteins

In mammals, the most common way of regulating ion channels is through neurotransmitters or hormones acting via G-protein-coupled receptors. GIRK channels are among the most extensively studied ion channels activated by G-proteins. (Dascal, 2001)G protein-coupled receptors make up the largest family of membrane-bound receptor proteins in eukaryotic cells. More than 800 different genes in humans are known to code for GPCRs. These receptors have been found in numerous tissues and are responsible for a wide range of physiological processes. (Wootten et al., 2018)

G proteins are vital for downstream signaling because they are responsible for converting ligand binding on the cell surface into responses inside the cell. These proteins are heterotrimers consisting of α-, β- and γ-subunits. (Hamm, 1998) There are 5 Gβ (GNB1 – GNB5) and 12 Gγ (GNG1 – GNG12) genes in the human genome, leading to diversity regarding structure and function of the different $G\beta_x\gamma_x$ subtypes. (Tennakoon et al., 2021b)

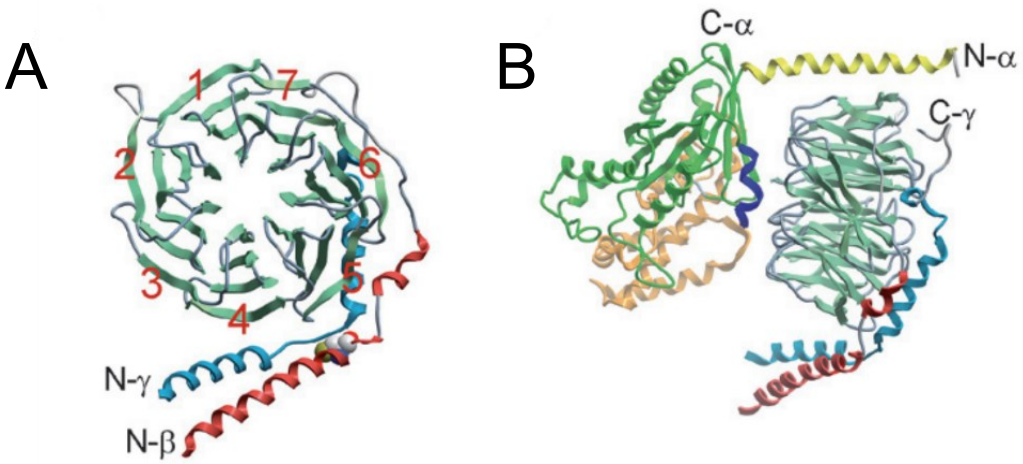

Figure 2 G protein structure. (A) Gβγ crystal structure. The propeller blades are numbered 1-7. Gβ terminus in shown in red interacting with Gγ shown in blue. **(B)** Heterotrimeric G protein structure representing the two interaction points of Gα with Gβγ. The N-terminal α-helix interacting with blade 1 is presented in yellow and the switch II region of Gα which is in interaction with the top of the propeller is displayed in dark blue. (Smrcka, 2008)

The β-subunits arrange into a β-propeller, with each of the seven propeller blades composed of four-stranded β-sheets. An α-helical domain is formed by the first 57–70 amino acids at the N-terminus of the β-propeller. This helix interacts tightly with the γ-subunit (Figure 2A). The Gα subunit contains two structural units that can both interact with Gβγ at different sites. Firstly, the α-helix at the N-terminus of Gα interacts with the side of blade 1 of the β-propeller (Figure 2B, yellow). Secondly, the switch II region of Gα, which undergoes conformational changes in reaction to GTP binding, interacts with the upper side of the β-propeller (Figure 2B, dark blue). (Smrcka, 2008)

1.3.1 GPCR induced channel activation

After a ligand (e.g. a neurotransmitter or a drug) binds to the extracellular side of the cell, the GPCR is stimulated and catalyzes the exchange of guanosine diphosphate (GDP) for guanosine triphosphate (GTP) on the α-subunit at the cytoplasmic side. Following the GDP-to-GTP exchange on Gα, Gβγ disassembles from the complex and becomes free to react with other cell structures. Once dissociated, the subunits can stimulate their target. In the case of GIRK channels, Gβγ binds directly to the channel, leading to the activation of the GIRK channel. (Figure 3) (Wang et al., 2014)

Many G protein interaction sites are located on the external side of e.g. a GIRK at the cytosolic domain, along an interface that is established by two neighboring subunits. Sequences from the C- and N-termini from different subunits play a crucial role in forming this interface. It has been confirmed that an interaction between these termini is important for

the gating and structure of GIRK channels. Within this interaction site, there is a hydrophobic pocket which also contributes to Gβγ-dependent activation. When activated, a conformational change takes place in the C- and N-termini. Some amino acids in the transmembrane segment form the ion gate, which changes its structure upon activation, subsequently opening the channel. (Lüscher and Slesinger, 2010) This allosteric effect opens and closes the pore by widening or narrowing the cytosolic outlet. Furthermore, this effect adapts permeation and gating at the selectivity filter. (Dascal, 2001)

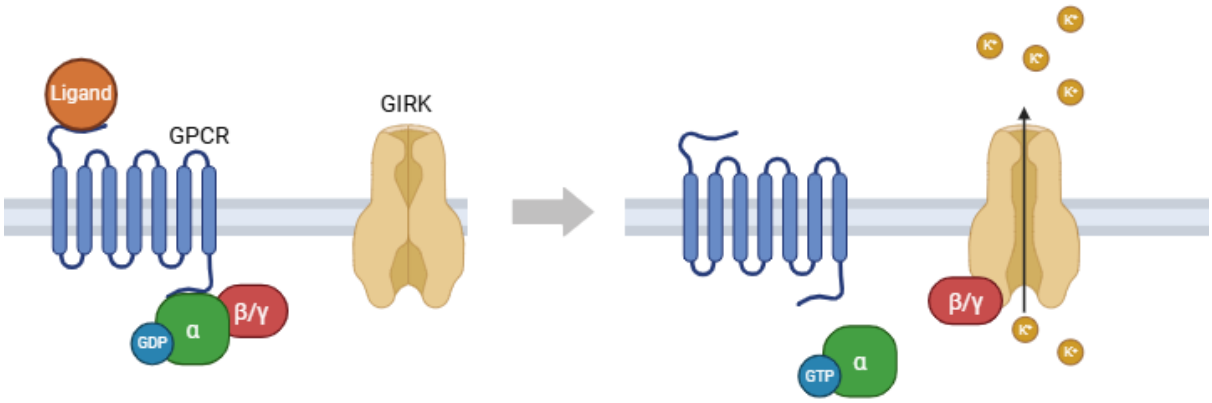

Figure 3 GIRK activation via GPCR. The complex GPCR-Gα(GDP)βγ is activated by a ligand binding to a G-protein-coupled receptor. Due to the activation, an exchange of GDP to GTP at the Gα-subunit occurs that leads to disassociation of Gβγ from Gα. Gβγ then binds to GIRK leading to activation and opening of the channel. (Wang et al., 2014)

It is confirmed that rather Gβγ than Gα is involved in GIRK channel stimulation. (Dascal, 2001) The importance of Gα in GIRK gating and the amount of impact this subunit has on the signal specificity stays unclear so far. (Peleg et al., 2002) As the interaction site of Gβγ for binding to GIRK overlaps with the interface for connecting with Gα, it is clear that the two subunits must separate from each other. (Dascal and Kahanovitch, 2015)

To support G protein activity, modifications to the subunits are essential. For example, prenylation at the C-terminus of Gγ appears to impact the plasma membrane affinity and signaling activity of Gβγ. It has been demonstrated that the greater the affinity for the plasma membrane, the more effective the signaling and therefore the activation of effectors. (Tennakoon et al., 2021a) The attached geranylgeranyl group points towards the membrane, functioning as an anchor that stabilizes the entire GIRK-Gβγ complex. (Whorton and MacKinnon, 2013)

1.4 M101V variant

The key focus of this work is the M101V mutation. The amino acid Methionine in position 101 is replaced with Valine (p.M101V). (Revah-Politi et al., 2020) This substitution genuinely does not affect the hydrophilicity. Both methionine and valine are considered aliphatic amino acids. Strictly speaking, an aliphatic side chain only contains carbon and hydrogen atoms. This considered, valine is definitely a member of this group. Methionine does also contain a sulfur atom, but since this is connected to a methyl group, making it less reactive, methionine is considered aliphatic too. Aliphatic side chains tend to be non-reactive and are therefore barely involved in protein function, but they are important for substrate recognition, as hydrophobic amino acids play a vital role in binding hydrophobic ligands.(Betts and Russell, 2003)

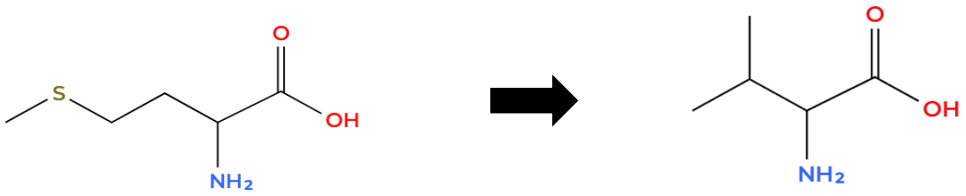

Figure 4 Substitution of methionine to valine in position 101. As both amino acids are aliphatic, the hydrophilicity fundamentally remains unchanged. (Betts and Russell, 2003)

1.4.1 GNB1 patients reported with M101V

There are two reported individuals with M101V mutation. The first one is a 19 year old, male European. Like all patients he suffers from GDD. In addition he has epileptic outbreaks and some abnormalities can be found in his EEG and MRI. His muscle tone is normal and he does not show any dysmorphic features. Autism spectrum disorder and behavioral problems can be observes in this patient. (Petrovski et al., 2016)

The second individual carrying the M101V mutation is a 20 year old, mixed European and Filipino female. She is also diagnosed with GDD and had her first tonic clonic seizures at the age of 11. Hypotonia was observed at two years, in toddlerhood she had gross motor milestone delay and in childhood mildly low muscle tone. Additionally she suffers from autism. Developmental regression of language occurred at the age of two and now she is non-verbal with significant receptive language. (Petrovski et al., 2016)

In summary, the common features of patients with the M101V mutation are global development delay, seizures and developmental regression. (Petrovski et al., 2016)

1.4.2 Reported Interactions

The M101V mutation has been documented to impact the Gβ1 residue, which interacts with calcium channels and activates adenylyl cyclase 2, phospholipase C-β2 and G-protein-coupled receptors. (Petrovski et al., 2016)

Reddy et al. observed the influence of specific mutations in Gβ1 regarding protein expression and function. The level of surface expression of the plasma membrane-attached Gβ1 protein was found to be considerably lower in comparison to the wild type. Both values were assessed in in giant membrane patches. The decrease in expression may explain the small activation of GIRK2 observed in Xenopus oocytes by evaluating the whole-cell GIRK currents. (Reddy et al., 2021)

1.4.3 Effect on AC5

Adenylyl cyclase 5 (AC5) is stimulated by Gα and a small molecule called forskolin, but is also influenced by other signaling partners like Gβγ. It's main purpose is to produce cAMP, a second messenger in GPCRs. (Yen et al., 2024)

It was shown that half the amount of Gα was needed for more cAMP production if AC5 was previously incubated with Gβγ. This finding suggests that Gβγ plays a role in stabilizing AC5 in a state that is optimized for the interaction with Gα. Several mutations in Gβγ were reported to decrease the AC5 activation. Amino acid M101 in Gβ is shown to form hydrophobic bonds with amino acid M696 located in the C_{1b}-α_2 region of AC5. (Figure 5B) This region is considered to have an autoinhibitory impact on AC5. Therefore binding of Gβγ to C_{1b}-α_2 results in less inhibition of AC5, making the adenyl cyclase ready or catalysis. (Yen et al., 2024)

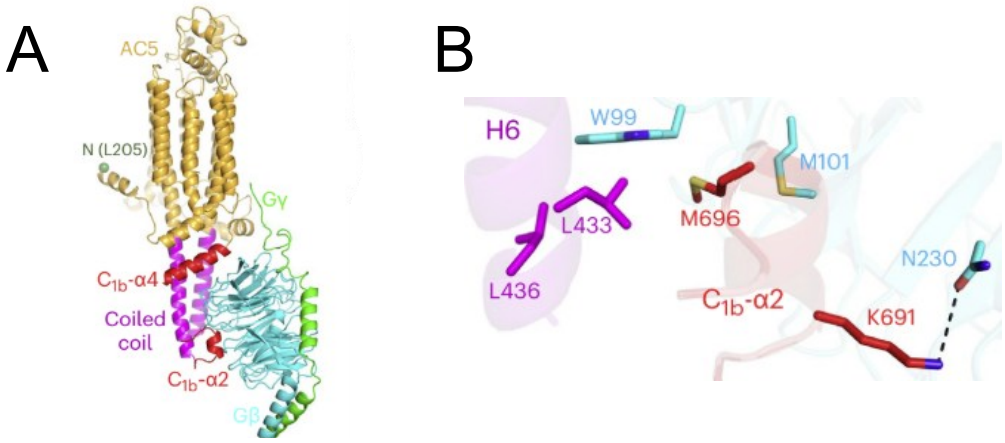

Figure 5 AC5 and Gβγ interaction. (A) AC5 structure is mostly shown in orange, but the interaction regions with Gβγ are shown in pink (coiled-coil domain) and red (C_{1b} domain). Gβ and Gγ are displayed in cyan and green, respectively. **(B)** Potential interactions between C_{1b}-α_2 region and Gβ. Gβ residue M101 is believed to interact with M696 of C_{1b}-α_2 domain in AC5. (Yen et al., 2024)

Various mutations in adenylyl cyclase 5 are connected to diseases including diabetes, central nervous system disorders and especially dyskinesia. These findings suggest that mutations in M101 could be linked to symptoms connected to the disorders mentioned above. (Yen et al., 2024)

1.5 Molecular dynamics (MD) simulation

In the last years molecular dynamics (MD) simulations gained a lot in importance in drug discovery and molecular biology. With these simulations, the movement of every atom in a protein over time can be calculated. Developments in simulation speed, accuracy and accessibility combined with the growing amount of structural data are responsible for the upgoing trend of using MD simulations in the scientific community. (Hollingsworth and Dror, 2018)

Several important biological processes like conformational change, protein folding and ligand binding can be investigated with MD simulations. The positions over time of all the atoms in the involved system can be captured at femtosecond temporal resolution. Additionally these simulations are vital for predicting how biomolecules will react to interferences including mutation, protonation and phosphorylation. (Hollingsworth and Dror, 2018) These simulations are often used in drug discovery for evaluating systems and understanding several molecular processes. (Bassani and Moro, 2023)

Previously, X-ray structures were the most common method for determining macromolecules utilized in molecular dynamics (MD) simulations. However, new techniques for determining structure have emerged, particularly in electron detection and imaging. This has enabled cryo-EM to gradually compete with X-ray. (Bai et al., 2015)

1.5.1 The Principle

In principle the idea behind a molecular dynamics simulation is to determine the positions of each and every atom in a specific biomolecular system, for instance: a protein with its surrounded water molecules and a lipid bilayer. With this information the force effecting each atom exerted by other atoms can be calculated. Fundamentally Newton's laws of motion are used for the specific prediction of the precise positions of the atoms as a function of time. In every time step all the forces that affect any atom are continuously calculated and these forces are then used to further analyze the positions and velocities of the atoms. The outcome is a trajectory that can be visualized in a three-dimensional movie, where the atomic configuration is simulated in femtosecond time steps. (Hollingsworth and Dror, 2018)

The forces in the simulation are typically calculated with the incorporation of a molecular mechanics force field. These force fields hold information about for example coulombic forces, terms that influence the preferred length of covalent bonds and terms that capture other interatomic interactions. (Hollingsworth and Dror, 2018)

Molecular interactions are estimated with the following empirical potential energy function:

$$\vec{F} = -\nabla U(\vec{r})$$

A force field combines a set of empirical potential energy functions and connected parameters for calculating the potential energy (U) as a function based on the molecular coordinates. This function consists out of non-bonded and bonded interactions, only considering pairwise interactions:

$$U(\vec{r}) = \sum U_{bonded}(\vec{r}) + \sum U_{non-bonded}(\vec{r})$$

Non-electrostatic, as well as electrostatic interactions between pairs of atoms are included in non-bonded terms. The non-electrostatic energy between a pair of non-bonded atoms or molecules is described by the Lennard-Jones potential:

$$V_{LJ}(r) = \frac{c_{12}}{r^{12}} - \frac{c_6}{r^6}$$

With r^{-12} representing the strong Puli repulsion that appears when electron orbitals overlap, and r^{-6} demonstrating weaker attractive forces between dipoles in the valence orbitals. Another common expression for the LJ potential is using the well depth (ϵ) and van der Waals radius (σ):

$$V_{LJ}(r) = 4\varepsilon \left[\left(\frac{\sigma}{r}\right)^{12} - \left(\frac{\sigma}{r}\right)^{6}\right], \quad C_{12} = 4\varepsilon\sigma^{12}, \quad C_6 = 4\varepsilon\sigma^6$$

To describe the electrostatic potential around a molecule, Coulomb's law can be applied:

$$V_{Elec} = \frac{q_i q_j}{4\pi\varepsilon_0\varepsilon_r r_{ij}}$$

Bonded terms include the bond potential $V_{Bond} = k_b(r_{ij} - r_0)^2$ (r_0: bond length, k_b: bond constant), the angle potential $V_{Angle} = k_\theta(\theta_{ijk} - \theta_0)^2$ (θ_0: bond angle, k_θ: force constant) and the torsion (dihedral) angle potential $V_{Dihed} = k_\phi(1 + cos(n\phi - \delta))$ (n: periodicity, δ: phase shift angle). (www.1)

Positions and velocities of the atoms can be determined by solving Newton's equations of motion over time. The outcome is a trajectory that captures configurations. (Adcock and McCammon, 2006)

Newton's second Law:

$$f_i(t) = m_i a_i(t) = -\frac{\partial V(x(t))}{\partial x_i(t)}$$

$f_i(t)$ denotes the net force that is appearing on atom i at time t. $a_i(t)$ represents the related acceleration and m_i characterizes the atom mass. (De Vivo et al., 2016).

1.5.2 Benefits

Compared to conventional experimental techniques, the main advantage of MD simulations is the ability to describe the position and motion of every atom at any given time, which is extremely difficult to achieve in traditional experiments. Furthermore, MD simulations offer flexibility in terms of protein conformation, mutations, ligands, post-translational modifications, protonation, temperature and voltage across membranes. All of these factors can be easily adapted and controlled within the simulation. By comparing a wild-type simulation with a perturbed-system simulation, the effects of different interferences can be measured. (Hollingsworth and Dror, 2018)

The increasing availability of graphics processor units (GPUs) is responsible for MD simulations to become widely accessible and reasonable in the point of costs. (De Vivo et al., 2016)

1.5.3 Limitations

Force fields have improved tremendously over the last few years, making the calculations more accurate. However, they still bring a specific grade of uncertainty, that has to be kept in mind. It has to be kept in mind that covalent bonds in a MD simulation neither bend nor break, which is not representing reality perfectly. Another limiting factor for MD simulations is the timescale. For ensuring stability, the simulation is supposed to be a few femtoseconds long in

maximum. Since a lot of biochemical processes of interest last up to nano- or microseconds, sometimes even longer, the computations tend to be extremely demanding. (Hollingsworth and Dror, 2018) More restrictions in molecular dynamics simulations include the electronic motions, that are not being taken to account, since we only look at the positions of atoms. Furthermore, force fields are limited even though their parameters can be adapted. Users should be aware of these restrictions to evaluate the accuracy of the MD simulation. (Bauer et al., 2022)

In addition to all these limitations there is a lot of expertise needed to meaningfully use molecular dynamics simulations. The barriers that have to be overcome are to figure out which problems can be addressed with MD simulations, to program the simulations for the specific cases and then to correctly interpret the data that is gained from the simulation. (Hollingsworth and Dror, 2018)

1.6 Free Energy Changes upon Amino Acid Mutation

A main goal in molecular design is to predict accurate changes of free energy upon amino acid mutation. This prediction is vital because free energy plays a central role in thermodynamics and kinetics. (Aldeghi et al., 2019)

The Gibbs energy, also known as free energy, denoted by G is a term used to describe thermodynamic processes under specific conditions. These include constant temperature and pressure, which are characteristic for biological processes. The Gibbs free energy is defined as G = H - TS. There, H is stands for the enthalpy of the system, T denotes the temperature and S refers to the entropy. This energy term is provides a basis for discussing equilibrium states. To determine whether a reaction is occurring spontaneously, one can examine the changes in Gibbs energy. If the free energy decreases during the process, as indicated by negative ΔG values, the reaction will proceed in the direction of converting the reactants into the product. In opposite, if the Gibbs energy increases, seen in positive ΔG values, the reverse reaction will happen spontaneously. If the system is in equilibrium, the Gibbs energy values are zero. (Atkins et al., 2018)

A lot of different methods have been established for the estimation of free energy changes. These approaches include alchemical free energy calculations, which are based on all-atom simulations using the Boltzmann distribution. The exchange of the amino acid in free energy calculations can be conducted reversibly and irreversibly, referred as equilibrium an non-equilibrium calculations. (Aldeghi et al., 2019)

The thermodynamic and kinetic properties, determined by the free energy surface of a system, offers information about biophysical processes like protein folding, protein-protein interaction and ligand binding. For further understanding, disordered conformations (unfolded systems) are referred to as State A and ordered conformations (folded systems) are termed State B. The relative equilibrium probability of the protein being rather in the unfolded State than in the folded state can be calculated with the difference between the free energy states:

$$\frac{p_A}{p_B} = \frac{e^{-\beta G_A}}{e^{-\beta G_B}} = e^{-\beta(G_A - G_B)} \qquad \Delta G = G_A - G_B = -k_\mathrm{B} T \ln \frac{p_A}{p_B}$$

G_A represents the free energy of the unfolded state, while G_B characterizes the free energy of the folded state. $\beta=1/k_BT$ with k_B being the Boltzmann constant and T describing the absolute temperature. (Aldeghi et al., 2019)

The maximum work conducted in the closed system can also be determined by the free energy difference, with the limitation of reversibility. The system has to be in an thermodynamic equilibrium state, where changes are infinitely small and slow. Any finite change applied to the system results in for example heat dissipation, forcing the system to be irreversible. According to the second law of thermodynamics, the work that is carried out during a process is equal or larger than the free energy changes:

$$\langle W(\tau) \rangle \geq \Delta G$$

with the limitation of a reversible process ($\tau \to \infty$). In opposite, for finite changes due to dissipative work, the coupling parameter λ is added to the equation. λ values range from 0 to 1 and are continually adapted at every time step. To calculate the work one can integrate the energetic cost that is required for the modification:

$$W(\tau) = \int_{\lambda=0}^{\lambda=1} \frac{\partial \mathcal{H}(\boldsymbol{x}, \boldsymbol{v}, \lambda)}{\partial \lambda} d\lambda$$

where H represents the Hamiltonian of the system, which is a function of the phase space coordinates (x), velocities (v) and the parameter λ. (Aldeghi et al., 2019)

For relating the non-equilibrium work to the free energy difference in equilibrium, Jarzynski established the following equlity:

$$\left\langle e^{-\beta W(\tau)} \right\rangle = e^{-\beta \Delta G}$$

This equation does require the non-equilibrium changes to start at an equilibrium state and is only looking at transitions in one direction. (Aldeghi et al., 2019)

To consider both directions, forward (λ: 0→1) and additionally reverse (λ: 1→0), the Crooks Fluctuation Theorem (CFT) can be used. CFT describes the relation of forward and reverse work on the free energy difference as:

$$\frac{P_f(W)}{P_r(-W)} = e^{\beta(W-\Delta G)}$$

with P_f (W) and P_r (W) representing the normalized probability distributions of work values gained from both transformation paths. The free energy difference can be calculated directly with the intersection between forward and reverse work distributions. (Aldeghi et al., 2019)

The so called BAR (Bennet's Acceptance Ratio) is another ΔG estimator, which does not need any kind of analytical approximation for the work distributions. The BAR calculates the free energy difference with the following equation:

$$\sum_{i=1}^{N_f} \frac{1}{1+\frac{N_f}{N_r} e^{\beta(W_i-\widehat{\Delta G})}} = \sum_{j=1}^{N_r} \frac{1}{1+\frac{N_r}{N_f} e^{-\beta(W_j-\widehat{\Delta G})}}$$

Here N_f and N_r embody the number of trajectories in forward and reverse direction. To solve this equation, one must proceed numerically using a Newton-Raphson or Nelder-Mead solver. (Aldeghi et al., 2019)

The initial step towards calculating the free energy difference is to determine the primary and final states of interest and furthermore to define the path connecting these states. For example we determine the initial state as unfolded protein and the final state as folded protein. To estimate the free energy difference between these states, one can measure the work that has to be conducted for unfolding the protein mechanically, by, for example, pulling the N- and C-termini of the protein apart. Since this calculation would require a lot of computational effort, it is more common to evaluate the changes in folding free energy ($\Delta\Delta G_{folding}$) by building a thermodynamic cycle. The approach of a thermodynamic cycle makes use of alchemical (non-physical) pathways that simulate smaller perturbations, which are computationally easier to converge. For instance, mutating a wild type protein alchemically into its mutant offers better results than unfolding both of them. (Aldeghi et al., 2019)

As shown in Figure 6, a wild-type protein can be mutated via alchemical pathway in both, folded and unfolded, states. With these non-physical transformations one can calculate $\Delta G_{Mutation\ Folded}$ and $\Delta G_{Mutation\ Unfolded}$ in order to recover the free energy difference $\Delta\Delta G_{Mutation}$

$_{Folding}$ ($\Delta G_{Mutation\ Folded}$ - $\Delta G_{Mutation\ Unfolded}$). Besides the less demanding non-alchemical pathway, the physical pathway can also be used to discover the free energy difference $\Delta\Delta G_{Mutation\ Folding}$ ($\Delta G_{Mut\ Folding}$ – $\Delta G_{WT\ Folding}$). It is a fact, that the unfolded state of protein is difficult to simulate

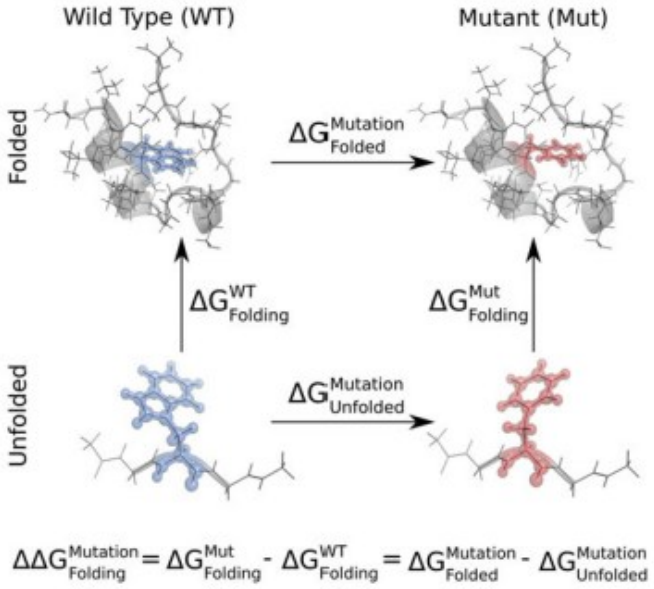

Figure 6 Thermodynamic cycle to calculate changes in free energy upon mutation. The horizontal transformations ($\Delta G_{Mutation\ Folded}$ and $\Delta G_{Mutation\ Unfolded}$) refer to the alchemical pathway, also called non-physical pathway. The vertical processes show the physical pathways ($\Delta G_{Mut\ Folding}$ and $\Delta G_{WT\ Folding}$), which are more computationally challenging to simulate. (Aldeghi et al., 2019)

due to its poor definition by nature. To evade this challenge, short fragments of the protein, typically tripeptides, are alternatively used instead of the whole protein in the unfolded state for evaluating the changes in the protein. Even though non-physical transformations are used for the calculation, the final result ($\Delta\Delta G$) refers to a physical process like folding. (Aldeghi et al., 2019)

The calculated free energy change upon amino acid mutation provides information about the stability of a protein. (Pancotti et al., 2022) If a mutation has destabilizing effects the value will be positive ($\Delta\Delta G>0$), while a stabilizing mutation will result in negative values ($\Delta\Delta G<0$). (Aldeghi et al., 2019)

Pathogenic GNB1 variants can interfere with several steps in G-protein signaling, including dimer stability, interaction with Gα, and binding to downstream effectors such as GIRK channels or AC5. In this work, the focus lies on the earliest point at which dysfunction may arise — the structural and thermodynamic stability of the Gβ1γ2 dimer itself.

2 Objective

Mutations in the Gβ1 subunit are responsible for the rare and severe disease called GNB1 Encephalopathy. To investigate the consequences of the specific mutation M101V, Molecular dynamics (MD) simulations were conducted. With these simulations the impact of the mutation in the pathologic Gβ1γ2 is demonstrated.

This work serves as fundament for understanding the effects of the mutation in Gβ1γ2 dimer on a molecular level. It can be considered for finding therapeutic approaches for treating GNB1 encephalopathy caused by the mutation M101V.

In the molecular dynamics simulation M101V is implemented in the G-protein, so that conformational changes in the protein structure can be visualized. The aim is to gain further information into the pathophysiology of GNB1.

For specifying the amount of impact the mutation has on the Gβ1γ2 subunit, following steps were conducted:

- Construction of a simulation system with mutation M101V included in Gβ1γ2 subunit based on PDB 4KFM
- Running non-equilibrium molecular dynamics simulations ranging from 50 to 200 ps for the tripeptide model and protein model of wild type and mutant Gβ1γ2 to analyze and compare the interactions
- Calculation of free energy changes upon the M101V mutation for a better understanding of the thermodynamic effects triggered by the pathogenic variant, especially regarding protein-protein interactions to estimate the stability of the protein complex
- Extension of MD simulation run 3 to 250 ns and further analysis of trajectories with focus on parameters like RSMF and RSMD

These investigations offer a groundwork to understand structural as well as functional impacts of the M101V mutation in the Gβ1γ2 complex.

3 Materials and Methods

3.1 Software

These molecular dynamics simulations were carried out with GROMACS version 2022.3. (Abraham et al., 2015)

LINUX Ubuntu version 2.04.6. is the operating system on which GROMACS was installed. (Van Der Spoel et al., 2005)

3.2 Preparation

The Gβγ subunit used for the MD simulations is based on PDB structure 4KFM, which contains a GIRK2 channel tetramer, and the attached four Gβ1γ2 subunits. It was prepared with CHARMM-GUI. The mutation M101V in the G subunit was generated with http://pmx.mpibpc.mpg.de/ . Methionine in position 101 is replaced with Valine with the pmx site. (Jo et al., 2008)

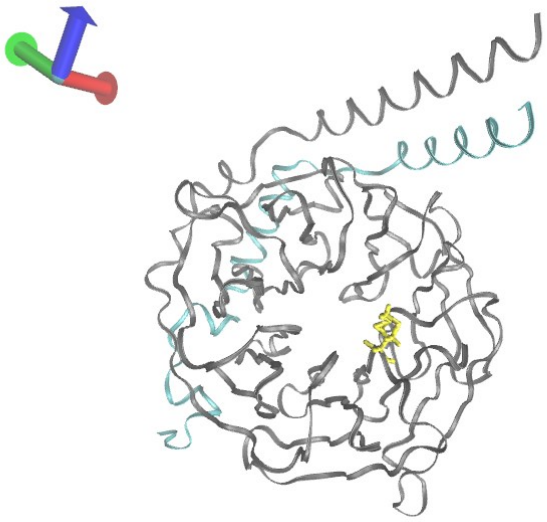

Figure 7 Gβ1γ2 complex extracted from 4KFM with mutant M101V highlighted in yellow color. Gβ1 shown in grey and Gγ2 in cyan. Structure created with VMD.

The force field that was used to asses all atoms speed and location over time is Amber99SB*ILDN. (Salomon-Ferrer et al., 2013) It's purpose is to calculate the dependence of the energy on the coordinates of the atoms. (González, 2011) The simulation was conducted for a protein in water system (TIP3P), which is known to be deliver data reasonably consistent with the experimental results. The ion concentration (Na+, Cl-) in the MD calculation was 0.15 mol/l. (Jorgensen et al., 1983)

3.3 Protocols

For calculating the free energy the following steps were conducted: energy minimization, NVT (constant number of particles, volume and temperature = isothermal-isosochoric) and NPT (constant number of particles, pressure and temperature = isothermal-isobaric) solvent equilibrium, production of MD (10 nanoseconds), and non-equilibrium MD (50-200 ps). The energy minimization step is to make sure the geometry is appropriate and the system exhibits no steric clashes. The outcome is a low in energy, relaxed structure. Putting the solvent in a favorable state regarding temperature, pressure and orientation with the solute is essential to avoid the system collapsing. After this step all atoms were in a starting position ready for the simulation. For the MD the restraints for the positions of the atoms were released and a 10 ns simulation is conducted. (www.2) The fist 2 ns were dismissed as equilibrium time. During the last 8 ns, 100 frames (one every 80 ps) were obtained. These frames offer an equilibrium collection of starting conformations for the non-equilibrium transitions. The working values for the transition (WT => M101V and M101V => WT) were gathered. With the use of the Crooks fluctuation theorem the free energy difference between both states was calculated followed by the determination of the free energy using Bennet`s Acceptance Ratio estimator. All steps were performed for 5 runs in total. (Aldeghi et al., 2019)

Run 3 was extended to 250 ns followed by RMSD and RMSF calculations with GROMACS. The root mean square deviation (RMSD) is a tool for comparing two structures. RMSD values give information about the quality of simulations and are used for clustering conformations. (Pitera, 2014) Its definition is the spatial difference between the atoms in two static structures. (Knapp et al., 2011) Another analyzation tool is the root mean square fluctuation (RMSF), which measures the variation in space of an atom or molecule over time from a reference position. It is considered an important flexibility index. (Song et al., 2024)

The simulations were performed on servers of the Vienna Scientific Cluster (VSC).

4 Results

The primary aim of this study was to understand the structural and dynamic effects of the mutation from methionine to valine in position 101. Molecular dynamics simulations were conducted for the investigation. Structural information of Gβ1γ2 was obtained from the Protein Data Bank (PDB ID: 4KFM). The results demonstrating the impact of the M101V mutation in Gβ1γ2, which is one of many mutations linked to a disease called GNB1 encephalopathy, are shown in the results chapter and will be described in more detail in the discussion section.

With the MD simulation data, free energy changes upon amino acid mutation (ΔΔG) were estimated. Further analysis of an extended MD run include RMSD and RMSF calculations.

Table 1 presents all simulation results for the tripeptide in summary and table 2 shows the same for the Gβ1γ2 subunit:

Run	**ΔG (kJ/mol)**
Run 1	-78,67 ± 0,33
Run 2	-76,74 ± 0,26
Run 3	-80,24 ± 0,34
Run 4	-78, 49 ± 0,34
Run 5	-79,13 ± 0,38

Table 1 Overview of the MD runs for the tripeptide that were carried out

Run	**ΔG (kJ/mol)**
Run 1	-70,74 ± 1,11
Run 2	-73,33 ± 0,63
Run 3	-74,91 ± 0,96
Run 4	-72,24 ± 0,76
Run 5	-81,32 ± 0,71

Table 2 Summarized results for the MD simulations in Gβ1γ2.

4.1 Free energy changes upon M101V for the tripeptide

With NEMD (non-equilibrium molecular dynamics) simulations 5 histograms, 1 for each run, were generated for the M101V tripeptide. These diagrams are snapshots demonstrating the transformation WT ⇔ M101V. The forward (WT => M101V) and backward (M101V => WT) transition work values are displayed on the left side of the plot. The right side shows the distribution for these values. For calculating the free energy difference the two distribution curves have to offer an intersection. The ΔG values calculated using the BAR (Bennet acceptance ratio) can be found on the top right part in each histogram.

Run 1	ΔG = -78,67 ± 0,33 kJ/mol	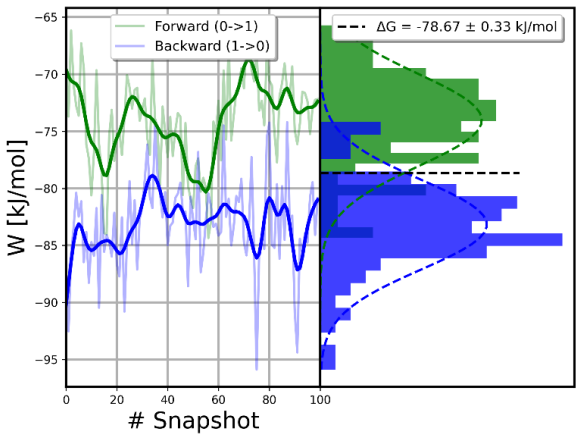
Run 2	ΔG = -76,74 ± 0,26 kJ/mol	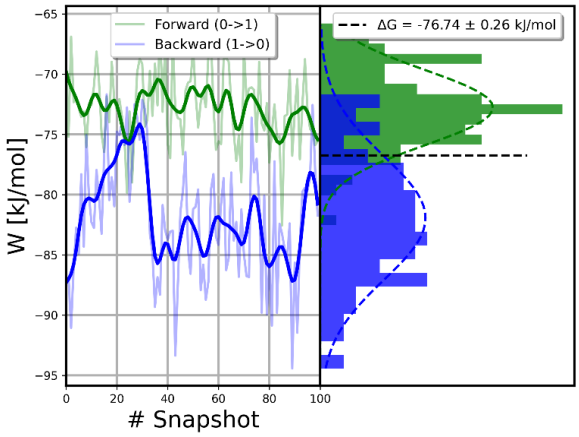

Run 3	ΔG = -80,24 ± 0,34 kJ/mol	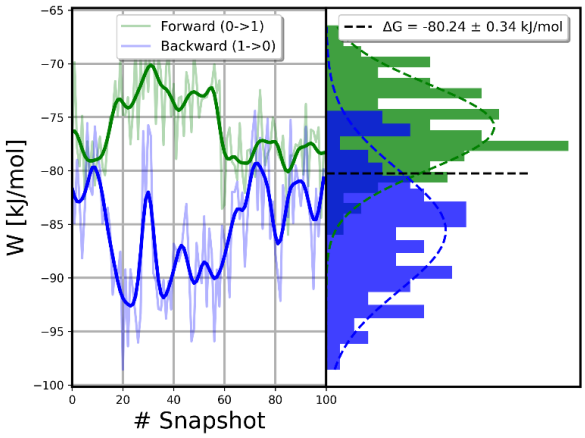
Run 4	ΔG = -78, 49 ± 0,34 kJ/mol	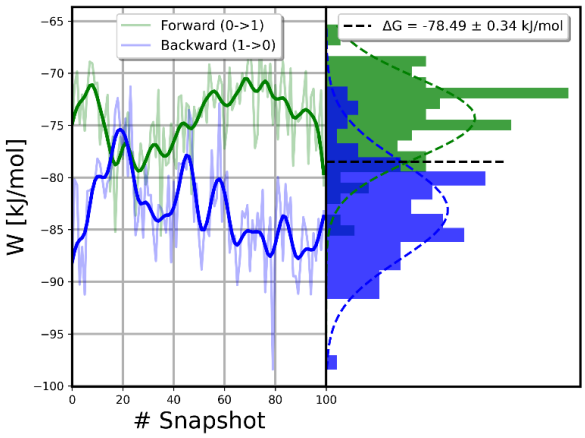
Run 5	ΔG = -79,13 ± 0,38 kJ/mol	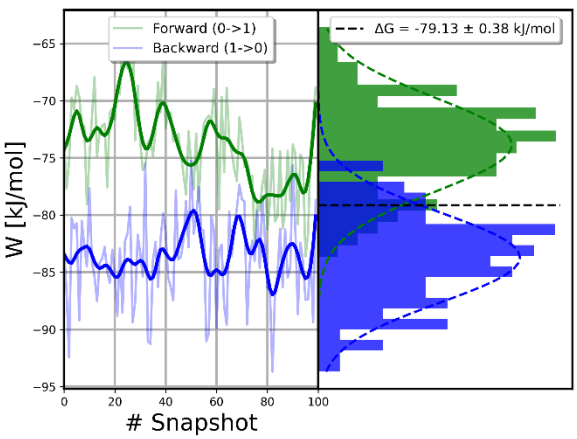

Table 3 Plots demonstrating the free energy calculation upon M101V mutation in the tripeptide. *Left:* Forward (green, WT => M101V) and backward (blue, M101V => WT) transition work values. *Right:* Distribution curves for the work values. The intersection demonstrates the change in free energy.

Based on the five free energy changes values, the average free energy of the tripeptide system was calculated:

$$\Delta G_{tripep}^{avg} = \frac{-78{,}67 + -76{,}74 + -80{,}24 + -78{,}49 + -79{,}13}{5} = -78{,}65\ kJ/mol$$

4.2 Free energy changes upon M101V in Gβ1γ2

Table 4 displays the results for the free energy changes for the Gβ1γ2 subunit. The same methodology (NEMD and BAR) as for the tripeptide was used. The obtained diagrams also show the work values on the left and the distribution of these values on the right side. The determination of the free energy difference was also based on the intersection of both distributions, as described for the tripeptide.

Run 1	ΔG = -70,74 ± 1,11 kJ/mol	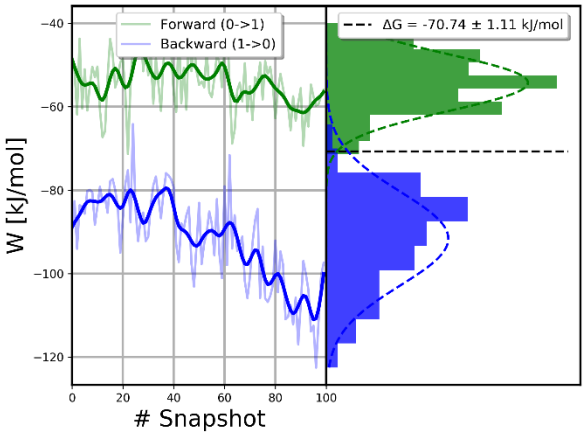
Run 2	ΔG = -73,33 ± 0,63 kJ/mol	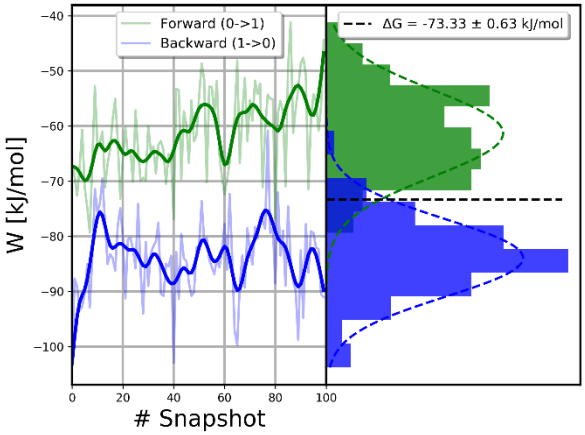

Run 3	ΔG = -74,91 ± 0,96 kJ/mol	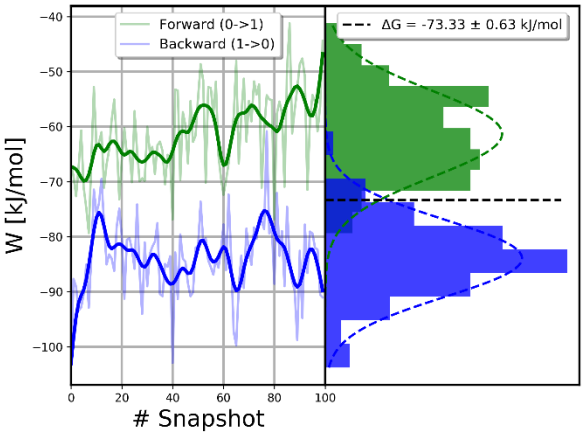
Run 4	ΔG = -72,24 ± 0,76 kJ/mol	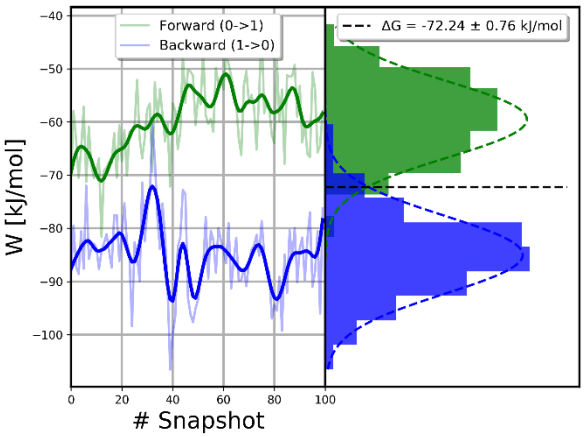
Run 5	ΔG = -81,32 ± 0,71 kJ/mol	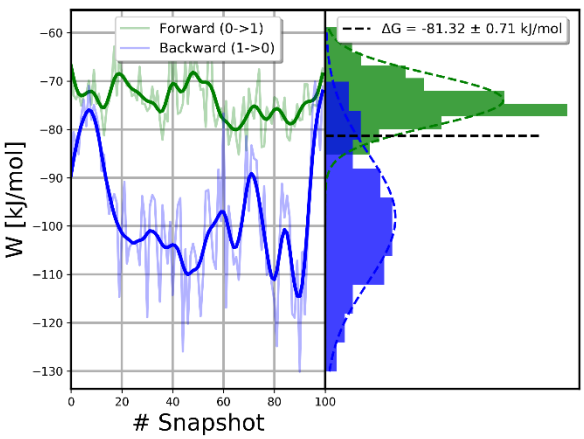

Table 4 Plots displaying the free energy calculation upon M101V mutation in the Gβ1γ2 subunit. *Left:* Forward (green, WT => M101V) and backward (blue, M101V => WT) transition work values. *Right:* Distribution curves for the work values. The intersection corresponds to the change in free energy.

4.3 ΔΔG calculations

The ΔΔG values for all five MD runs were calculated with the use of the following formula provided by Aldeghi et al.:

$$\Delta\Delta G_{folding}^{mutation} = \Delta G^{protein} - \Delta G_{tripep}^{avg}$$

An overview of the calculated ΔΔG values for each run is shown below in Table 5.

Run	**ΔΔG (kJ/mol)**
1	7,91
2	5,32
3	3,74
4	6,41
5	-2,67

Table 5 Summarized results for ΔΔG in Gβ1γ2

The average ΔΔG value for the M101V mutation were calculated:

$$\Delta\Delta G_{folding\ avg}^{mutation} = \frac{7{,}91 + 5{,}32 + 3{,}74 + 6{,}41 + -2{,}67}{5} = 4{,}15\ kJ/mol$$

The average ΔΔG value for the mutation of methionine to valine in position 101 is 4,15 kJ/mol. This result indicates that the M101V mutation has a slightly destabilizing effect on the Gβ1γ2 structure.

4.4 Root mean square deviation (RMSD)

With the extension of run 3 to 250 ns, the backbone for WT and M101V was monitored. The evaluated RMSD values for both simulations are illustrated in Figure 7.

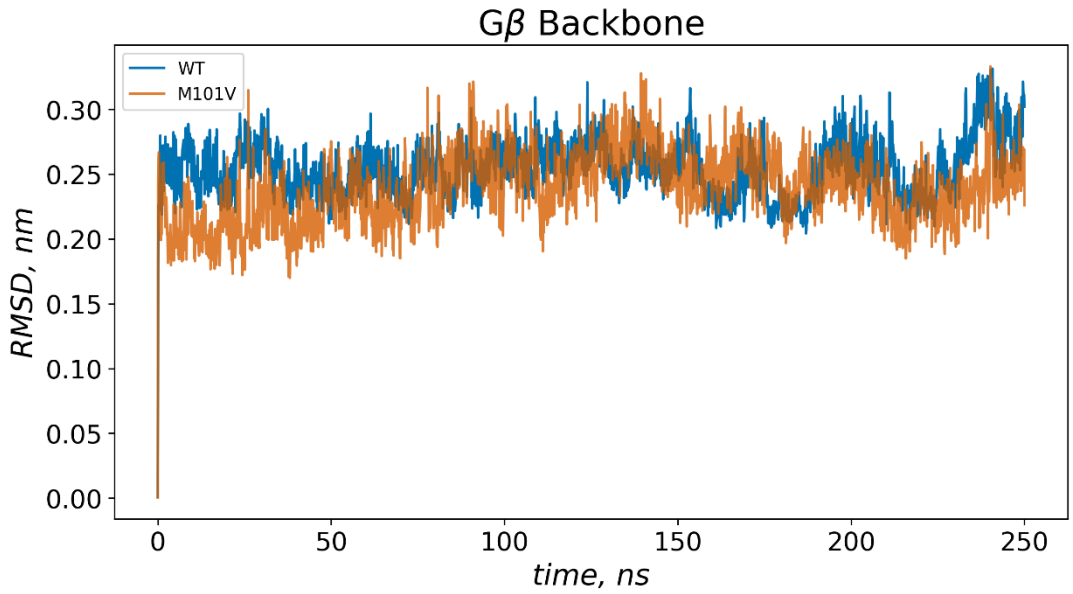

Figure 8 RMSD comparison of WT (blue) and M101V (orange) Gβ subunits within the Gβ1γ2 complex.

Both curves RMSD values fluctuate around 0,20 and 0,30 nm and stayed stable throughout the whole process. The M101V mutant exhibited comparable values to the wild-type, suggesting that the mutation maintains the overall structure of the protein. Therefore functional effects of this variant are most likely due to local or dynamic changes, not because of huge structural perturbations.

4.5 Root mean square fluctuation (RMSF)

The backbone RMSF values were also calculated for wild-type and mutation. The root mean square fluctuation gives information about local flexibility of different residues. Figure 8 displays the RMSF values for the Gβ1-M101V-mutant and the Gβ1-WT.

Both RMSF profiles show similar patterns. Around residue 100, which is the region where the mutation is embedded, there does not occur a difference in flexibility between WT and M101-mutant. Overall these results support the findings of the RMSD, indicating maintained structural stability.

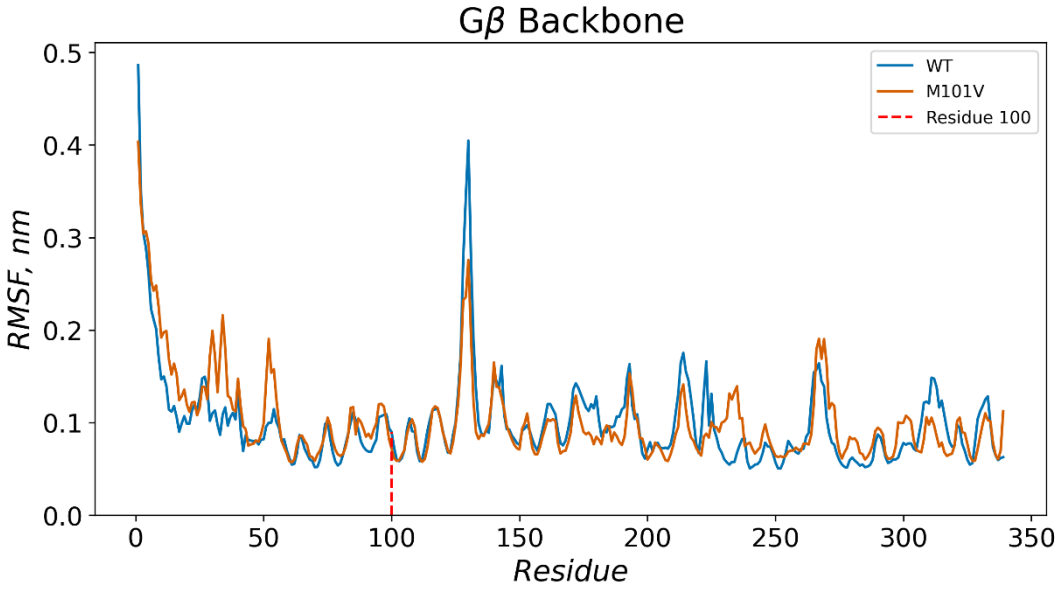

Figure 9 RMSF comparison of WT (blue) and M101V (orange) Gβ subunits within the Gβ1γ2 complex. The red line marks the region where the mutation occurs.

4.6 Hydrogen Bonds

Additionally nonbonded interaction between WT or M101V with surrounding water was measured. As seen in Figure 11 the V101 consistently shows weaker interaction with water compared to the M101 wild type.

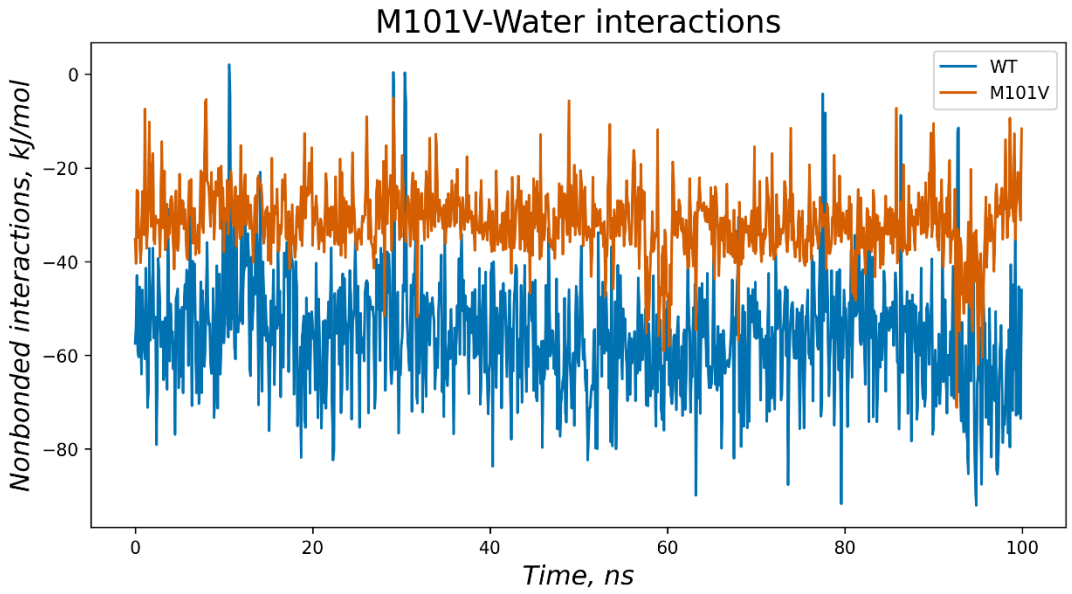

Figure 10 Nonbonded interaction energy between WT (blue) and M101 (orange) and surrounded water molecules.

This effect is probably based on the fact that methionine is a little more polar in comparison to very hydrophobic valine. The reduction in this solvation energy suggests a slight decrease in local polarity around residue 101 which may lead to influences side-chain packing or protein-protein interaction.

4.7 Residue interaction

The following figures compare the nonbonded interaction energies between residue 101 (wild-type = methionine or mutant = valine) and neighbouring residues in Gβ1γ2, decomposed into total, Lennard-Jones (LJ) and Coulombic (electrostatic) contributions.

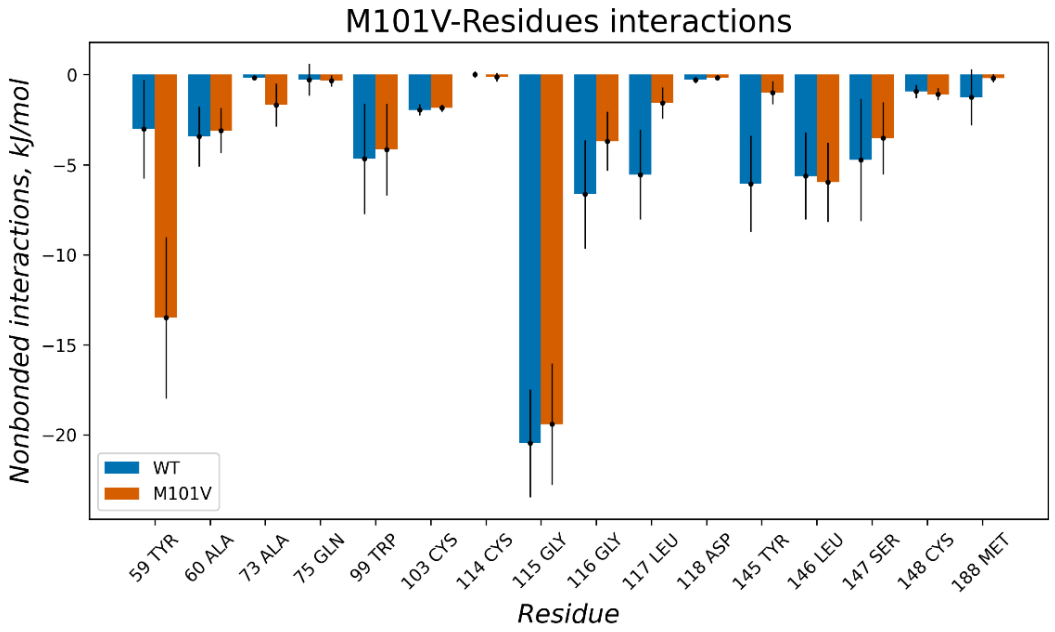

Figure 12 Total nonbonded interactions. WT and M101V show similar interaction with surrounding residues.

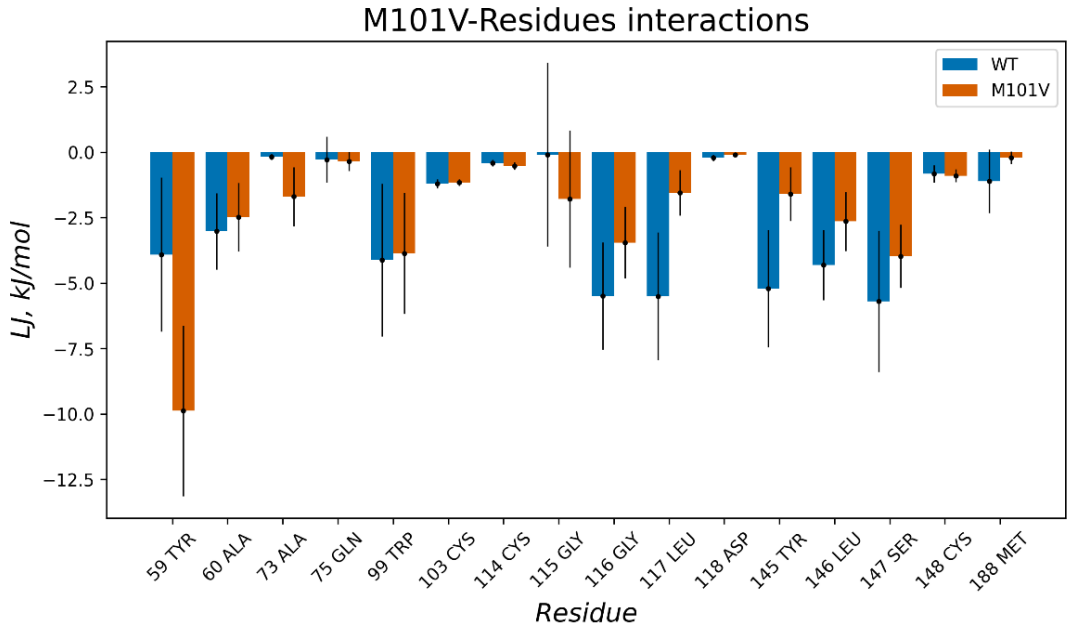

Figure 11 Lennard-Jones interactions. Van der Waals interaction energy between WT or mutant with other residues is comparable.

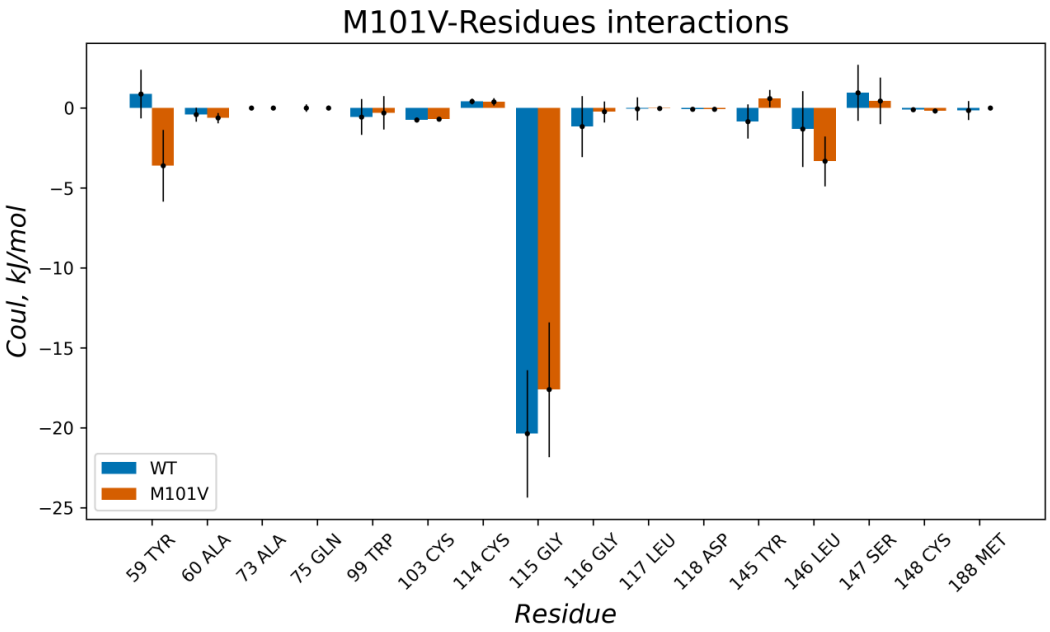

Figure 13 Coulombic interactions. Minor electrostatic contributions were also calculated to be quite similar.

Overall, both variants exhibit very similar interaction patterns. A slight redistribution of non-bonded interactions between WT and M101V is observed at amino acids 59TYR, 116GLY, 117LEU, 145TYR. These results suggest that the M101V mutation may slightly alter the balance of hydrophobic or polar interactions locally but does not contribute significantly to the residue network around.

5 Discussion

The aim of this study was to explore the structural and thermodynamic consequences of the M101V mutation in the Gβ1γ2 complex. This part of a G protein is associated with a rare neurodevelopmental disorder called GNB1 encephalopathy.

By combining non-equilibrium free energy calculations with extended molecular dynamics simulations for the wild-type and M101V mutant Gβ1γ2 dimers, this work provides an assessment of how the substitution of methionine by valine at amino acid position 101 affects protein stability, structural dynamics and local interactions. The crystal structure 4KFM provided by the Protein Data Bank was used as a template.

The calculated ΔΔG value of 4,15 kJ/mol indicates that the M101V mutation exerts a mild destabilizing effect on the Gβ1γ2 structure. Although small in extent, this value is consistent across four out of five simulation runs and therefore reflects a reproducible trend. Destabilization in this range rarely leads to major unfolding events, but may influences local conformation or protein-protein interfaces. The ΔΔG value obtained aligns with the expectation that the exchange of methionine to valine, which is slightly less polar, potentially weakens stability, however, not to a huge extent. This may explain the intermediate phenotypes presented by the two patients in comparison to other, probably more disruptive, variants.

RMSD values for WT and mutant remained stable throughout the whole simulation and exhibited nearly identical trajectories, fluctuating between 0,20 and 0,30 nm. This indicates that the mutation does not cause significant structural rearrangements of the Gβ1 subunit within the Gβ1γ2 dimer. Equally for the RMSF, the profiles for the wild-type and M101V mutant were extremely similar. The critical region surrounding the mutation around residue 100, did not display increased local flexibility in the mutant. Together, these findings suggest that M101V preserves the backbone structure and overall dynamics of the protein. Consequently, any functional impairment liked to this mutation does not seem to appear due to major structural destabilization.

Analysis of nonbonded interactions with water revealed an clear difference between the two systems. The wild-type methionine residue exhibited stronger solvation energies than the mutant valine residue. This is consistent with the sightly higher polarity of methionine in comparison to valine. The mutation therefore results in reduced local polarity. This observation fits into the context that residue 101 participates in interactions with neighbouring residues and potentially contributes to effector binding (e.g. AC5).

However, looking at the residue-residue interactions, it was revealed that both WT and M101V display very similar patterns for total nonbonded, Lennard-Jones and Coulombic energies. This suggests that the overall packing and intramolecular contacts around residue 101 remain largely preserved.

The structural effects of M101V seem to be subtle, but even small alterations in the hydrophobic microenvironment can influence the interactions between Gβ1γ2 and other effectors, such as AC5 or GIRK channels. Although the simulations in this study do not assess effector binding, the observed molecular changes are consistent with previously reported reductions in surface expression and reduced GIRK2 activation in M101V-expressing systems.

This molecular profile is compatible with the moderate but clinically significant symptoms observed in the two reported patients and supports the idea, that GNB1 encephalopathy can arise not only from huge structural disruptions, but also from minor perturbations in effector regulation.

6 Conclusion

This work provides a molecular characterization of the GNB1 M101V mutation through MD simulations and free energy calculations. With this, an initial step towards understanding the structural and functional effects of this mutation was taken.

The results demonstrate that M101V induces a small but consistent destabilization of the Gβ1γ2 complex and alters the local hydrophobic environment without causing large-scale structural changes. The overall fold and dynamic behavior of Gβ1 remains intact, while free energy analyses reveal subtle modifications that may influence effector interactions. In the case of this mutation, interactions with GIRK channels or AC5 might be influenced, contributing to the neurological phenotype observed in the affected individuals.

The simulations in this thesis address the first step in the chain of events through which the M101V mutation may influence G-protein function, namely the intrinsic stability of the Gβ1γ2 dimer. Since only a mild destabilization was observed and the overall fold remained intact, the mutation's functional effects may occur at later stages, such as altered interaction with Gα or reduced binding to effectors like GIRK channels or AC5. Future studies should therefore extend the simulations to these complexes to determine whether the subtle local changes detected here translate into measurable differences in signaling. These results may offer deeper insights and support the development of precise therapeutic strategies.

Finally, it is essential to differentiate between the different mutations in GNB1. To increase our understanding of the disease-causing mutation in relation to the phenotypes, more studies regarding other mutations are essential for finding specific treatment options for the predominant mutation type.

7 References

Abraham, M.J., Murtola, T., Schulz, R., Páll, S., Smith, J.C., Hess, B., Lindahl, E., 2015. GROMACS: High performance molecular simulations through multi-level parallelism from laptops to supercomputers. SoftwareX 1–2, 19–25. https://doi.org/10.1016/j.softx.2015.06.001

Adcock, S.A., McCammon, J.A., 2006. Molecular dynamics: survey of methods for simulating the activity of proteins. Chem. Rev. 106, 1589–1615. https://doi.org/10.1021/cr040426m

Aldeghi, M., de Groot, B.L., Gapsys, V., 2019. Accurate Calculation of Free Energy Changes upon Amino Acid Mutation. Methods Mol. Biol. Clifton NJ 1851, 19–47. https://doi.org/10.1007/978-1-4939-8736-8_2

Atkins, P.W., Keeler, J., De Paula, J., 2018. Atkins' physical chemistry. Oxford University Press.

Bai, X., McMullan, G., Scheres, S.H.W., 2015. How cryo-EM is revolutionizing structural biology. Trends Biochem. Sci. 40, 49–57. https://doi.org/10.1016/j.tibs.2014.10.005

Bassani, D., Moro, S., 2023. Past, Present, and Future Perspectives on Computer-Aided Drug Design Methodologies. Molecules 28, 3906. https://doi.org/10.3390/molecules28093906

Bauer, P., Hess, B., Lindahl, E., 2022. GROMACS 2022.3 Manual. https://doi.org/10.5281/zenodo.7037337

Betts, M.J., Russell, R.B., 2003. Amino Acid Properties and Consequences of Substitutions, in: Bioinformatics for Geneticists. John Wiley & Sons, Ltd, pp. 289–316. https://doi.org/10.1002/0470867302.ch14

Da Silva, J.D., Costa, M.D., Almeida, B., Lopes, F., Maciel, P., Teixeira-Castro, A., 2021. Case Report: A Novel GNB1 Mutation Causes Global Developmental Delay With Intellectual Disability and Behavioral Disorders. Front. Neurol. 12. https://doi.org/10.3389/fneur.2021.735549

Dascal, N., 2001. Ion-channel regulation by G proteins. Trends Endocrinol. Metab. 12, 391–398. https://doi.org/10.1016/S1043-2760(01)00475-1

Dascal, N., Kahanovitch, U., 2015. Chapter Two - The Roles of Gβγ and Gα in Gating and Regulation of GIRK Channels, in: Slesinger, P.A., Wickman, K. (Eds.), International Review of Neurobiology, Structure to Function of G Protein-Gated Inwardly Rectifying (GIRK) Channels. Academic Press, pp. 27–85. https://doi.org/10.1016/bs.irn.2015.06.001

De Vivo, M., Masetti, M., Bottegoni, G., Cavalli, A., 2016. Role of Molecular Dynamics and Related Methods in Drug Discovery. J. Med. Chem. 59, 4035–4061. https://doi.org/10.1021/acs.jmedchem.5b01684

González, M.A., 2011. Force fields and molecular dynamics simulations. Éc. Thématique Société Fr. Neutron. 12, 169–200. https://doi.org/10.1051/sfn/201112009

Hamm, H.E., 1998. The many faces of G protein signaling. J. Biol. Chem. 273, 669–672. https://doi.org/10.1074/jbc.273.2.669

Hemati, P., Revah-Politi, A., Bassan, H., Petrovski, S., Bilancia, C.G., Ramsey, K., Griffin, N.G., Bier, L., Cho, M.T., Rosello, M., Lynch, S.A., Colombo, S., Weber, A., Haug, M., Heinzen, E.L., Sands, T.T., Narayanan, V., Primiano, M., Aggarwal, V.S., Millan, F., Sattler-Holtrop, S.G., Caro-Llopis, A., Pillar, N., Baker, J., Freedman, R., Kroes, H.Y., Sacharow, S., Stong, N., Lapunzina, P., Schneider, M.C., Mendelsohn, N.J., Singleton, A., Loik Ramey, V., Wou, K., Kuzminsky, A., Monfort, S., Weisz Hubshman, M., Doyle, S., Iglesias, A., Martinez, F., Mckenzie, F., Orellana, C., van Gassen, K.L.I., Palomares, M., Bazak, L., Lee, A., Bircher, A., Basel-Vanagaite, L., Hafström, M., Houge, G., Group, C.R., Study, D.D.D., Goldstein, D.B., Anyane-Yeboa, K., 2018. Refining the phenotype associated with GNB1 mutations: Clinical data on 18 newly identified patients and review of the literature. Am. J. Med. Genet. A. 176, 2259–2275. https://doi.org/10.1002/ajmg.a.40472

Hollingsworth, S.A., Dror, R.O., 2018. Molecular Dynamics Simulation for All. Neuron 99, 1129–1143. https://doi.org/10.1016/j.neuron.2018.08.011

Jo, S., Kim, T., Iyer, V.G., Im, W., 2008. CHARMM-GUI: A web-based graphical user interface for CHARMM. J. Comput. Chem. 29, 1859–1865. https://doi.org/10.1002/jcc.20945

Jones, H.F., Morales-Briceño, H., Barwick, K., Lewis, J., Sanchis-Juan, A., Raymond, F.L., Stewart, K., Waugh, M.-C., Mahant, N., Kurian, M.A., Dale, R.C., Mohammad, S.S., 2019. Myoclonus-dystonia caused by GNB1 mutation responsive to deep brain stimulation. Mov. Disord. 34, 1079–1080. https://doi.org/10.1002/mds.27708

Jorgensen, W.L., Chandrasekhar, J., Madura, J.D., Impey, R.W., Klein, M.L., 1983. Comparison of simple potential functions for simulating liquid water. J. Chem. Phys. 79, 926–935. https://doi.org/10.1063/1.445869

Knapp, B., Frantal, S., Cibena, M., Schreiner, W., Bauer, P., 2011. Is an intuitive convergence definition of molecular dynamics simulations solely based on the root mean square deviation possible? J. Comput. Biol. J. Comput. Mol. Cell Biol. 18, 997–1005. https://doi.org/10.1089/cmb.2010.0237

Lohmann, K., Masuho, I., Patil, D.N., Baumann, H., Hebert, E., Steinrücke, S., Trujillano, D., Skamangas, N.K., Dobricic, V., Hüning, I., Gillessen-Kaesbach, G., Westenberger, A., Savic-Pavicevic, D., Münchau, A., Oprea, G., Klein, C., Rolfs, A., Martemyanov, K.A., 2017. Novel GNB1 mutations disrupt assembly and function of G protein heterotrimers and cause global developmental delay in humans. Hum. Mol. Genet. 26, 1078–1086. https://doi.org/10.1093/hmg/ddx018

Luo, H., Marron Fernandez de Velasco, E., Wickman, K., 2022. Neuronal G protein-gated K+ channels. Am. J. Physiol. Cell Physiol. 323, C439–C460. https://doi.org/10.1152/ajpcell.00102.2022

Lüscher, C., Slesinger, P.A., 2010. Emerging roles for G protein-gated inwardly rectifying potassium (GIRK) channels in health and disease. Nat. Rev. Neurosci. 11, 301–315. https://doi.org/10.1038/nrn2834

Lysozyme in Water [WWW Document], n.d. URL http://www.mdtutorials.com/gmx/lysozyme/05_EM.html (accessed 11.1.25).

Nasvytis, M., Čiauškaitė, J., Jurkevičienė, G., 2024. GNB1 Encephalopathy: Clinical Case Report and Literature Review. Medicina (Mex.) 60, 589. https://doi.org/10.3390/medicina60040589

Pancotti, C., Benevenuta, S., Birolo, G., Alberini, V., Repetto, V., Sanavia, T., Capriotti, E., Fariselli, P., 2022. Predicting protein stability changes upon single-point mutation: a thorough comparison of the available tools on a new dataset. Brief. Bioinform. 23, bbab555. https://doi.org/10.1093/bib/bbab555

Peleg, S., Varon, D., Ivanina, T., Dessauer, C.W., Dascal, N., 2002. G(alpha)(i) controls the gating of the G protein-activated K(+) channel, GIRK. Neuron 33, 87–99. https://doi.org/10.1016/s0896-6273(01)00567-0

Petrovski, S., Küry, S., Myers, C.T., Anyane-Yeboa, K., Cogné, B., Bialer, M., Xia, F., Hemati, P., Riviello, J., Mehaffey, M., Besnard, T., Becraft, E., Wadley, A., Politi, A.R., Colombo, S., Zhu, X., Ren, Z., Andrews, I., Dudding-Byth, T., Schneider, A.L., Wallace, G., Rosen, A.B.I., Schelley, S., Enns, G.M., Corre, P., Dalton, J., Mercier, S., Latypova, X., Schmitt, S., Guzman, E., Moore, C., Bier, L., Heinzen, E.L., Karachunski, P., Shur, N., Grebe, T., Basinger, A., Nguyen, J.M., Bézieau, S., Wierenga, K., Bernstein, J.A., Scheffer, I.E., Rosenfeld, J.A., Mefford, H.C., Isidor, B., Goldstein, D.B., 2016. Germline De Novo Mutations in GNB1 Cause Severe Neurodevelopmental Disability, Hypotonia, and Seizures. Am. J. Hum. Genet. 98, 1001–1010. https://doi.org/10.1016/j.ajhg.2016.03.011

Pitera, J.W., 2014. Expected Distributions of Root-Mean-Square Positional Deviations in Proteins. J. Phys. Chem. B 118, 6526–6530. https://doi.org/10.1021/jp412776d

Reddy, H.P., Yakubovich, D., Keren-Raifman, T., Tabak, G., Tsemakhovich, V.A., Pedersen, M.H., Shalomov, B., Colombo, S., Goldstein, D.B., Javitch, J.A., Bera, A.K., Dascal, N., 2021. Encephalopathy-causing mutations in Gβ1 (GNB1) alter regulation of neuronal GIRK channels. iScience 24, 103018. https://doi.org/10.1016/j.isci.2021.103018

Revah-Politi, A., Sands, T.T., Colombo, S., Goldstein, D.B., Anyane-Yeboa, K., 2020. GNB1 Encephalopathy. In: Adam, M.P., Feldman, J., Mirzaa, G.M., Pagon, R.A., Wallace, S.E., Amemiya, A. (Eds.), GeneReviews®. University of Washington, Seattle.

Salomon-Ferrer, R., Case, D.A., Walker, R.C., 2013. An overview of the Amber biomolecular simulation package. WIREs Comput. Mol. Sci. 3, 198–210. https://doi.org/10.1002/wcms.1121

Smrcka, A.V., 2008. G protein βγ subunits: Central mediators of G protein-coupled receptor signaling. Cell. Mol. Life Sci. 65, 2191–2214. https://doi.org/10.1007/s00018-008-8006-5

Song, X., Bao, L., Feng, C., Huang, Q., Zhang, F., Gao, X., Han, R., 2024. Accurate Prediction of Protein Structural Flexibility by Deep Learning Integrating Intricate Atomic Structures and Cryo-EM Density Information. Nat. Commun. 15, 5538. https://doi.org/10.1038/s41467-024-49858-x

Tennakoon, M., Senarath, K., Kankanamge, D., Chadee, D.N., Karunarathne, A., 2021a. A short C-terminal peptide in Gγ regulates Gβγ signaling efficacy. Mol. Biol. Cell 32, 1446–1458. https://doi.org/10.1091/mbc.E20-11-0750

Tennakoon, M., Senarath, K., Kankanamge, D., Ratnayake, K., Wijayaratna, D., Olupothage, K., Ubeysinghe, S., Martins-Cannavino, K., Hébert, T.E., Karunarathne, A., 2021b. Subtype-dependent regulation of Gβγ signalling. Cell. Signal. 82, 109947. https://doi.org/10.1016/j.cellsig.2021.109947

Van Der Spoel, D., Lindahl, E., Hess, B., Groenhof, G., Mark, A.E., Berendsen, H.J.C., 2005. GROMACS: Fast, flexible, and free. J. Comput. Chem. 26, 1701–1718. https://doi.org/10.1002/jcc.20291

Walsh, K.B., 2020. Screening Technologies for Inward Rectifier Potassium Channels: Discovery of New Blockers and Activators. SLAS Discov. 25, 420–433. https://doi.org/10.1177/2472555220905558

Wang, W., Whorton, M.R., MacKinnon, R., 2014. Quantitative analysis of mammalian GIRK2 channel regulation by G proteins, the signaling lipid PIP2 and Na+ in a reconstituted system. eLife 3, e03671. https://doi.org/10.7554/eLife.03671

Whorton, M.R., MacKinnon, R., 2013. X-ray structure of the mammalian GIRK2-βγ G-protein complex. Nature 498, 190–197. https://doi.org/10.1038/nature12241

Wootten, D., Christopoulos, A., Marti-Solano, M., Babu, M.M., Sexton, P.M., 2018. Mechanisms of signalling and biased agonism in G protein-coupled receptors. Nat. Rev. Mol. Cell Biol. 19, 638–653. https://doi.org/10.1038/s41580-018-0049-3

Yen, Y.-C., Li, Y., Chen, C.-L., Klose, T., Watts, V.J., Dessauer, C.W., Tesmer, J.J.G., 2024. Structure of adenylyl cyclase 5 in complex with Gβγ offers insights into ADCY5-related dyskinesia. Nat. Struct. Mol. Biol. 31, 1189–1197. https://doi.org/10.1038/s41594-024-01263-0

8 Internet references

www.1:https://computecanada.github.io/molmodsim-md-theory-lesson-novice/01-Force_Fields_and_Interactions/index.html (accessed 21.11.25)

www.2: Lysozyme in Water [WWW Document], n.d. URL http://www.mdtutorials.com/gmx/lysozyme/05_EM.html (accessed 11.1.25)